Skeletal Radiology (2019) 48:429–436
https://doi.org/10.1007/s00256-018-3049-7

SCIENTIFIC ARTICLE

3D-MRI versus 3D-CT in the evaluation of osseous anatomy in femoroacetabular impingement using Dixon 3D FLASH sequence

Mohammad Samim[1] · Nima Eftekhary[2] · Jonathan M. Vigdorchik[2] · Ameer Elbuluk[2] · Roy Davidovitch[2] · Thomas Youm[2] · Soterios Gyftopoulos[1]

Received: 21 June 2018 / Revised: 7 August 2018 / Accepted: 14 August 2018 / Published online: 4 September 2018

Abstract

Objective To determine if hip 3D-MR imaging can be used to accurately demonstrate femoral and acetabular morphology in the evaluation of patients with femoroacetabular impingement.

Materials and methods We performed a retrospective review at our institution of 17 consecutive patients (19 hips) with suspected femoroacetabular impingement who had both 3D-CT and 3D-MRI performed of the same hip. Two fellowship-trained musculoskeletal radiologists reviewed the imaging for the presence and location of cam deformity, anterior–inferior iliac spine variant, lateral center-edge angle, and neck–shaft angle. Findings on 3D-CT were considered the reference standard. The amount of radiation that was spared following introduction of 3D-MRI was also assessed.

Results All 17 patients suspected of FAI had evidence for cam deformity on 3D-CT. There was 100% agreement for diagnosis (19 out of 19) and location (19 out of 19) of cam deformity when comparing 3D-MRI with 3D-CT. There were 3 type I and 16 type II anterior–inferior iliac spine variants on 3D-CT imaging with 89.5% (17 out of 19) agreement for the anterior–inferior iliac spine characterization between 3D-MRI and 3D-CT. There was 64.7% agreement when comparing the neck–shaft angle (11 out of 17) and LCEA (11 out of 17) measurements. The use of 3D-MRI spared each patient an average radiation effective dose of 3.09 mSV for a total reduction of 479 mSV over a 4-year period.

Conclusion 3D-MR imaging can be used to accurately diagnose and quantify the typical osseous pathological condition in femoroacetabular impingement and has the potential to eliminate the need for 3D-CT imaging and its associated radiation exposure, and the cost for this predominantly young group of patients.

Keywords Femoroacetabular impingement · 3D MRI · 3D CT

Introduction

Femoroacetabular impingement (FAI) is caused by repetitive motion by an abnormal proximal femur and/or acetabulum during a terminal range of motion [1]. Patients with FAI are generally young and active, and have hip or groin pain, which is at its worst with prolonged sitting and with hip flexion and internal rotation [1]. The accurate diagnosis and characterization of the soft tissue and osseous pathological condition in FAI patients is paramount to initiating therapy and potentially altering the natural history of the disease [1–10].

The imaging algorithm for FAI patients typically begins with pelvic and hip radiographs to assess for the presence and degree of hip osteoarthritis in addition to abnormal bone morphology such as cam deformities, acetabular retroversion, and anterior inferior iliac spine (AIIS) hypertrophy [11–13]. The Dunn view, or elongated femoral neck view, is useful for defining the anterior–superior femoral head–neck junction, and has higher sensitivity than the cross table lateral in demonstrating a cam deformity [14]. A false profile view can also demonstrate anterior acetabular overcoverage. MRI is typically ordered to evaluate for the common soft-tissue injuries seen in FAI, including labral tears and cartilage degeneration [15, 16]. High-resolution CT imaging with 3D reconstructions can

✉ Mohammad Samim
mohammad.samim@nyumc.org

[1] Department of Radiology, New York University Langone Medical Center, 333 East 38th street, New York, NY 10016, USA

[2] Department of Orthopedic Surgery, NYU Langone Orthopedic Hospital, 301 East 17th Street, New York, NY 10003, USA

be utilized for more accurate evaluation of the bony pathomorphology of FAI. 3D-CT is of particular importance to both surgeon and radiologist for its accurate depiction and quantification of the abnormal bone morphology, allowing for preoperative planning and understanding of the underlying FAI biomechanics [17–22]. Although effective, this imaging algorithm can predispose the typical young FAI patient population to an increased radiation dose from radiographic and CT studies and the higher costs associated with obtaining both MRI and CT.

Magnetic resonance imaging with 3D reconstructions has already been shown to be an accurate means of evaluating shoulder anatomy and bone pathological conditions in the setting of shoulder instability [23, 24]. Were 3D-MRI to demonstrate similar effectiveness in evaluating the bony pathological condition of FAI, this would obviate the need to perform CT. The aim of this study was to determine if 3D-MRI of the hip can be used to accurately demonstrate femoral and acetabular morphology in the setting of FAI when compared with 3D-CT. We hypothesized that there would be no significant difference when comparing these two types of 3D imaging. The amount of radiation that was spared following the introduction of 3D-MRI at our institution was also studied.

Materials and methods

Institutional review board approval was obtained, and informed consent was waived for the retrospective Health Insurance Portability and Accountability Act-compliant study.

We performed a retrospective review of 17 consecutive patients (15 with unilateral studies, and 2 with bilateral studies, for a total of 19 hips) who underwent both CT and MRI of the same hip at our institution over a 9-month period with the following inclusion criteria:

1. Patients suspected of having FAI based on physical education
2. No prior hip surgery
3. Patients undergoing CT and MR examination with 3D reconstructions of the same hip within a 6-month period

Imaging techniques

The MRI studies were performed on a 3-T MR scanner (Siemens Medical; see Table 1 for a summary of MRI sequences and parameters). In addition to routine sequences, each MRI examination included an axial 3D dual echo-time T1-weighted FLASH sequence with Dixon-based water–fat separation with the following parameters: TR 10, TE 2.4, field of view of 200 mm, acquired voxel size of 1.0 × 1.0 × 1.4 mm, reconstructed voxel size 1.0 × 1.0 × 1.0 mm, flip angle 145 °, matrix 192 × 100, bandwidth of 350, and a slice thickness of 1 mm. All patients were imaged with an 18-channel body phase array coil. The Dixon imaging acquisition time was 3:28 min. We used a previously described post-processing technique to create the 3D MR reconstructions [23, 24]. The 3D reconstructions were done at the original time of the examination by the specialized technician in our 3D imaging laboratory. The reconstructed 3D images were subsequently sent to PACS for evaluation and measurement.

Each CT examination was performed on a 40-slice scanner (Siemens Medical) with a protocol consisting of volumetric 3-mm acquisitions through the hip and the following parameters: 120 kV, 280 mAs, pitch 0.9, 0.6-mm collimation, and a smooth algorithm. The axial images then underwent manual segmentation, generating 3D reconstructions of the hip (Tera Recon software [4.4.5.36.2068]).

Imaging evaluation

Two fellowship trained musculoskeletal radiologists (11 and 6 years of experience respectively), who were blinded to the patient's clinical history, performed a consensus review of the 3D-MRI and 3D-CT reconstructions of each hip. These reviews were performed in a random fashion in two separate sessions, separated by 2 weeks to ensure that the 3D-MR and

Table 1 Summary of MRI sequences and parameters

Sequence	Plane	Slice thickness (mm)	TR (ms)	TE (ms)	Field of view (mm × mm)	Acquisition matrix
STIR	Coronal	5	4,000	35	350	192 × 256
PD FS	Sagittal	3	2,900–3,000	22–35	160	256 × 256
T2 FS	Axial	3	3,500–,4500	40	200	224 × 256
PD	Coronal	3	3,000–3,500	34–38	160	192 × 256
PD	Oblique axial	3	2,900–3,000	22–35	200	224 × 256
Dixon	Axial	1	10	2.4	200	192 × 100

STIR short tau inversion recovery, *PD* proton density, *FS* fat-suppressed, *TE* echo time, *TR* repetition time

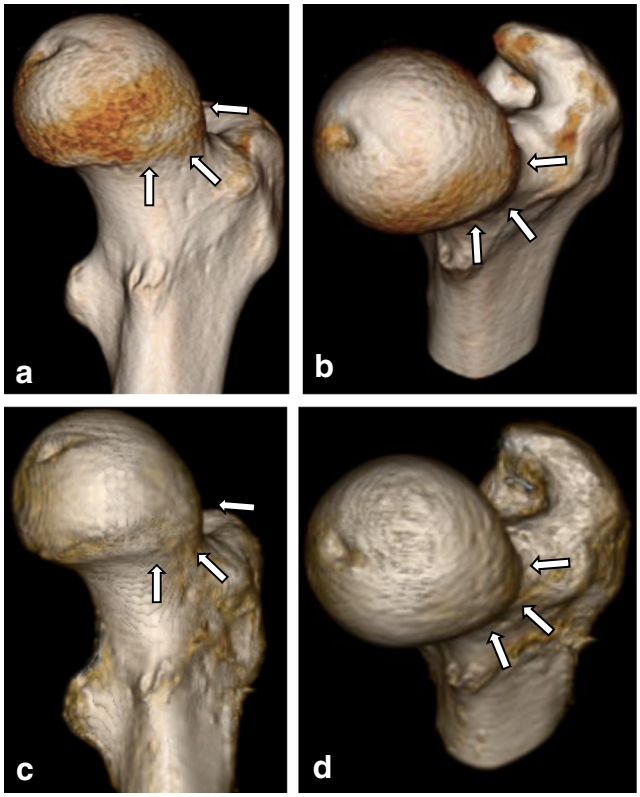

Fig. 1 A 34-year-old man with anterior left hip pain. Cam deformity and its location. **a**, **b** 3D volume rendered CT and **c**, **d** MRI images of the left femur demonstrate a large anterior cam deformity (*arrows*)

3D-CT models of the same patient were not reviewed in the same session. Three sets of 3D models were obtained including a femur only model following computerized subtraction of the acetabulum, an acetabulum only model following computerized subtraction of the femur, and a combined femur and acetabulum (hip) model. For each study, the femoral model was evaluated for:

1. The presence of a cam deformity as reduced offset at the femoral head–neck junction
2. The cam location, anterior or posterior at the femoral head–neck junction (Fig. 1)
3. Femoral neck–shaft angle (NSA) formed by the axis of the femoral shaft and the femoral neck axis (Fig. 2)

The measurement on the femoral model is performed following tilting of the model in the sagittal plane so that the long axis of the femoral shaft becomes parallel to the vertical axis of the image and rotating it until two thirds of the transverse width of the lesser trochanter, measured from the base to the tip of the trochanter, comes into profile. The center of the femoral head and the waist of the neck were determined to define the femoral neck axis. The long axis of the femur shaft was defined by a line connecting the centers of two circles placed around the outer margins of the sub-trochanteric femur at two positions: the center of the upper circle was positioned at the lower margin of the lesser trochanter and the lower circle was drawn 2 cm below the first within the confinement of the image (Fig. 2) [25].

Each 3D acetabulum and hip model was assessed for the AIIS morphology variant according to the classification proposed by Hetsroni et al. [26] and the lateral center edge angle (LCEA) (Figs. 3 and 4). To measure the LCEA, the transverse axis of the pelvis was determined using a line passing through the center of the femoral heads. If the contralateral hip was not included in the study field of view, an attempt was made to determine the true transverse plane of the pelvis using the scout coronal images and transferring the axis line to the 3D images [25]. To draw the circle

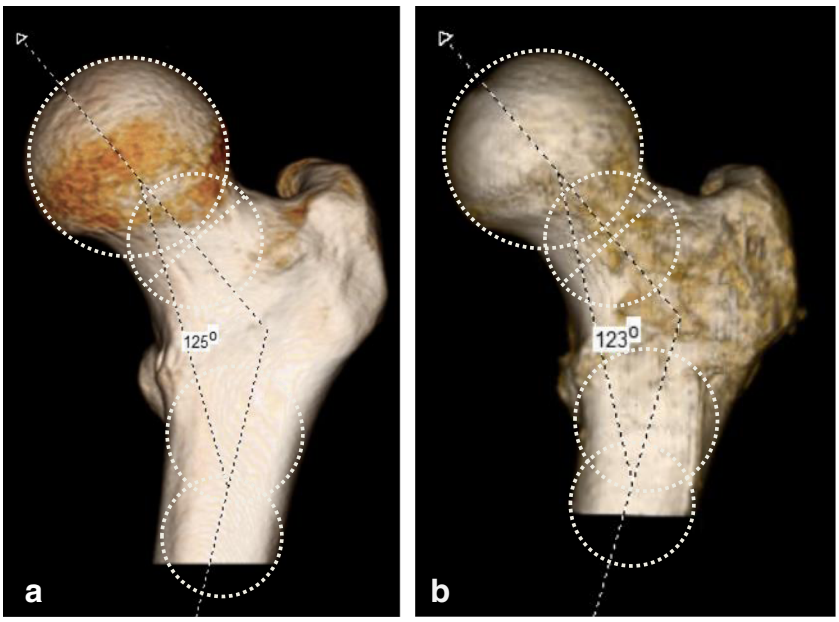

Fig. 2 A 41-year-old woman with left hip pain. Femoral neck–shaft angle measurement. **a** 3D volume rendered CT and **b** MRI images of the left hip demonstrate the femoral neck–shaft angle following definition of the femoral neck axis and drawing two circles in the femur to define the long femoral axis. Note that two thirds of the length of the lesser trochanter is visible on the 3D images

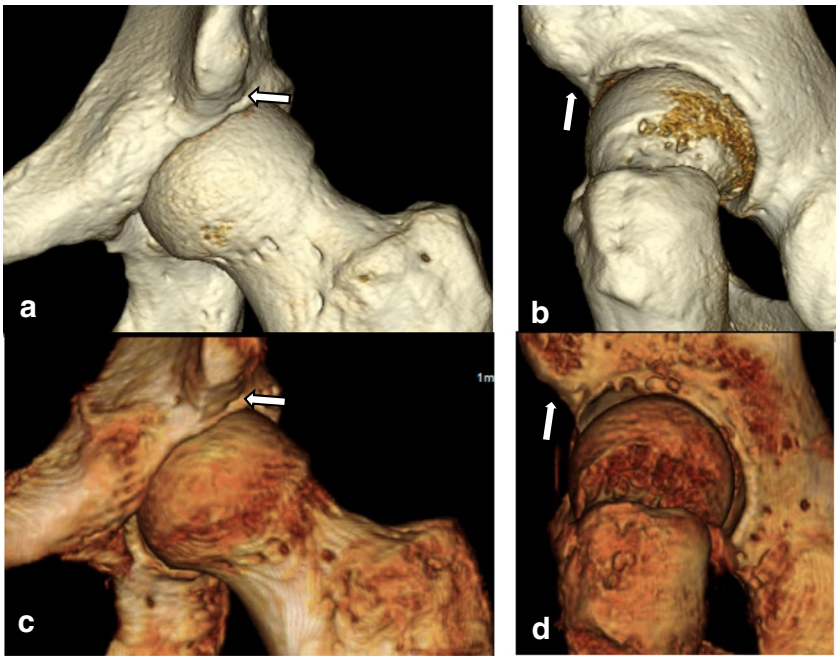

Fig. 3 A 27-year-old woman with left hip pain. Anterior–inferior iliac spine morphology. **a**, **b** 3D volume rendered CT and **c**, **d** MRI images of the left hip demonstrate type II anterior–inferior iliac spine as images rotate in two different views (*arrows*)

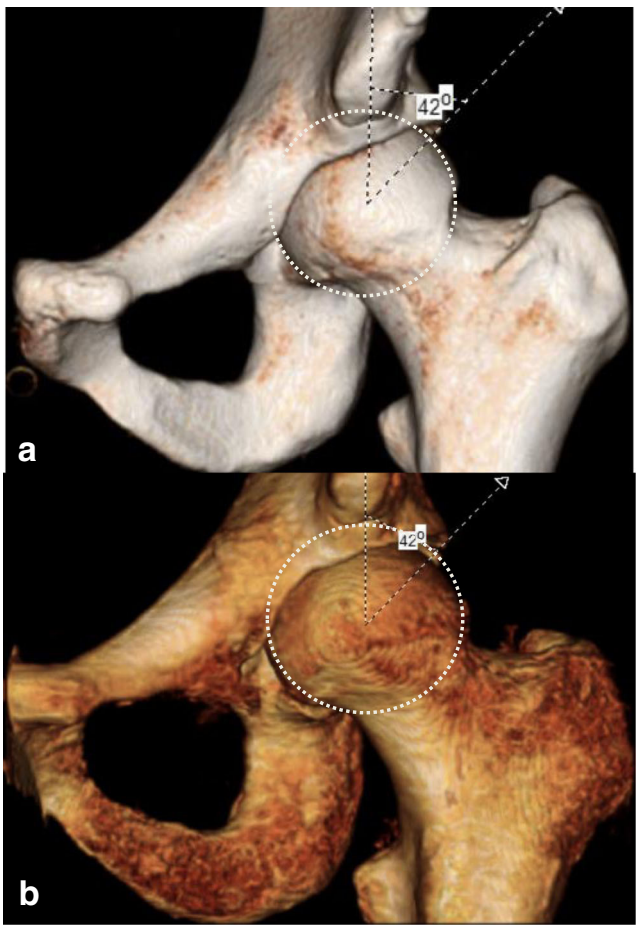

Fig. 4 A 41-year-old woman with left hip pain. Lateral center-edge angle measurement. **a** 3D volume rendered CT and **b** MRI of the left hip demonstrate measurement of the lateral center-edge angle from the center of the femoral head determined by the best fit circle around the femoral head to the edge of lateral bone

of best fit around the femoral head for determining the center of the femoral head, the circle was initially defined on the femur model and applied to the hip model, as the femoral head is partially covered by the acetabulum. The LCEA was measured as the angle between a line perpendicular to the transverse axis of the pelvis and a second line extending from the center of the femoral head to the lateral margin of the acetabular roof. All measurements discussed represent two-dimensional measurements performed on 3D volume rendered images. The findings on the 3D-CT reconstructions were considered the reference standard.

Radiation dose

To assess the amount of radiation spared following introduction of 3D-MRI at our institution, we performed a separate retrospective review of a different cohort who had orders for 3D CT or MRI reconstructions for FAI submitted to our 3D laboratory from April 2012 to March 2016. The ability to create 3D MRI reconstructions was first introduced at our institution in 2012, whereas 3D CT reconstructions were available before that year. We reviewed the orders and corresponding patient medical records for the following information: age, gender, date of study, and clinical indication. The estimated spared effective dose was recorded for each patient who avoided CT by having MRI, based on the dose computed by the scanner for the CT hip protocol for FAI patients.

Statistical analysis

Statistical analysis included simple kappa coefficients to measure inter-rater agreement. Reliability measurements were

calculated using the Shrout–Fleiss intraclass correlation coefficients for continuous parameters and weighted Kappa for categorical parameters.

Results

There were a total of 17 patients (19 hips), 9 male and 8 female, with a mean age of 37 (range 17–63 years) who met our inclusion criteria. All 17 patients had a clinical diagnosis of FAI. Two patients had bilateral hip imaging. Three sets of 3D imaging models, as discussed for both MRI and CT, were obtained for all patients. The mean total post-processing time required to produce 3D-MRI reconstructions was approximately 7 min (5.2–9 min) for each study, and 6.5 min (4–8.3 min) compared with that of 3D-CT reconstructions.

All 17 patients with suspected FAI had evidence of an anterior cam deformity on 3D-CT imaging (Fig. 1). There was 100% agreement in terms of presence (19 out of 19) and location (19 out of 19) of the cam deformity when comparing the interpretations made on 3D-MRI with those made on 3D-CT. The simple kappa coefficients for cam presence and locations were both 1. Relative to CT as the reference standard, MRI had an accuracy of 89.5% (17 out of 19) for AIIS characterization, with a simple kappa coefficient of 0.46 between MRI and CT. There were 3 type I and 16 type II AIIS variants on 3D CT imaging (Fig. 2). There were 2 type II variants called on 3D-MRI that were type I on 3D-CT.

There was 64.7% (11 out of 17) agreement for femoral NSA and 64.7% (11 out of 17) agreement for LCEA measurements between 3D-MRI and 3D-CT. We defined the angle measure from MRI as accurate relative to CT when the values produced by MRI and CT for the same hip differed by no more than 5°. The data used for analysis are summarized in Table 2. The NSA in MRI for 2 patients was not measured because there was not enough coverage of the femoral shaft to reliably determine the femoral shaft axis. In 2 patients, the LCEA on MRI was not included because the true transverse axis of the pelvis could not be determined, as the contralateral hip was not included and the coronal scout images were suboptimal.

There were a total of 185 reconstructions for FAI patients, 155 3D-MRI and 30 3D-CT between April 2012 and March 2016. On average, there were 36 3D-MRI and 7 3D-CT reconstructions each year. The use of 3D-MRI spared all 155 patients from CT study and each patient an average radiation effective dose of 3.09 mSV, for a total reduction of 479 mSV.

Discussion

Hip preservation procedures, particularly hip arthroscopy, are being performed with an almost exponential increase in the number of procedures performed annually [22]. The most common cause of reoperation in hip arthroscopy is the failure to adequately address the osseous pathological condition [22, 27]. Therefore, adequate preoperative understanding and characterization of the osseous pathological condition is paramount to ensuring optimal outcomes for the FAI patient population.

Table 2 Summary of imaging measurement data

Patient	Femoral neck shaft angle		Coronal center edge angle		Cam presence		Cam location		AIIS type	
	CT	MRI	CT	MRI	CT	MRI	CT	MRI	CT	MRI
1	137	134	46	–	1	1	1	1	2	2
2	135	134	40	37	1	1	1	1	1	2
3	129	133	33	33	1	1	1	1	2	2
4	130	137	27	37	1	1	1	1	2	2
5	138	136	26	26	1	1	1	1	2	2
6	125	136	41	34	1	1	1	1	2	2
7	125	127	25	22	1	1	1	1	2	2
8	138	136	42	38	1	1	1	1	1	1
9	136	–	36	33	1	1	1	1	2	2
10	129	128	38	37	1	1	1	1	1	2
11	140	133	17	24	1	1	1	1	2	2
12	139	133	31	28	1	1	1	1	2	2
13	132	134	31	24	1	1	1	1	2	2
14	134	135	24	18	1	1	1	1	2	2
15	131	139	18	22	1	1	1	1	2	2
16	133	130	36	37	1	1	1	1	2	2
17	136	–	55	–	1	1	1	1	2	2
18	136	134	55	46	1	1	1	1	2	2
19	131	124	35	33	1	1	1	1	2	2
Mean	133.3	133.1	34.0	31.1						

Our findings suggest that 3D-MRI can be used as an alternative to 3D-CT for the evaluation of the FAI patient population. There was 100% agreement for the diagnosis and location of cam deformities and good agreement for defining the AIIS type. These variables guide treatment for this cohort and are both paramount in the surgeon's preoperative plan. In addition, there was fair agreement for the femoral NSA and LCEA measurements.

At most centers, high-resolution CT with 3D reconstructions is ordered to better understand and visualize abnormal osseous anatomy. The 3D-CT is thought to provide a more accurate representation of the osseous anatomy compared with 2D imaging and is thus more helpful in preoperative planning [21, 28]. However, CT exposes patients to additional radiation and carries the cost of additional cross-sectional imaging. At our institution, the hip preservation surgeons have decreased their use of preoperative CT, and base their evaluation and preoperative planning on 3D-MRI alone. This change in our practice has resulted in a considerable reduction in effective radiation dose (479 mSV) in this predominantly young population since the introduction of 3D-MRI.

One previous study described a different technique for producing 3D-MRI of the hip to evaluate a patient with FAI [29]. The authors used a 3D gradient echo (VIBE) sequence based on magnetic resonance arthrography (MRA) on one patient to produce the reconstructions and design a virtual 3D model to quantify the maximal range of hip motion [29]. They performed a 3D dynamic evaluation for the visualization and quantification of the impingement zones between the femur and acetabulum. The authors manually marked and stored bony structures in each individual MRA slice, resulting in increased post-processing time. This increase in time is not reported in their study. In another case report, Chhabra et al. compared 3D-CT and 3D-MRI in a case of FAI with chronic acetabular rim fracture [30]. They used 3D isotropic spin echo type imaging on a 3-T scanner with bone segmentation and surface rendering using the available CT software and reported 27 min of additional processing time required (7 min for 3D image acquisition and 20 min for image reconstruction) [30]. Neither of these studies assessed the FAI morphology. It bears noting that at our institution, the total post-processing time for producing 3D-MRI reconstructions is approximately 7 min per study, nearly identical to that of 3D-CT reconstructions. The small amount of time needed to produce these 3D MR reconstructions has been crucial to the successful incorporation of this imaging technique into our workflow.

Our study suggests that 3D MR hip reconstructions may be sufficient to replace preoperative 3D-CT scans in the evaluation of the young patient with suspected FAI. We found fair agreement for the NSA and LCEA measurements between 3D-MRI and 3D-CT. The LCEA has been shown to reliably quantify excessive acetabular coverage (pincer deformity) when the angle is above 39–40° [6, 11, 22, 31, 32] and hip dysplasia [33], with values less than 20–25° [33–36]. In addition, NSA is one of the parameters that assesses the position and interaction of the proximal femur and the acetabulum. Reduced femoral NSA (coxa vara) in the presence of cam deformity can result in earlier impingement and FAI symptoms with flexion–internal rotation [37, 38]. It is unclear why there was less agreement between femoral NSA and LCEA measurements compared with other assessments of osseous morphology. One potential reason is the lack of established measurement methods specific to 3D models, as these two measurements are typically performed on radiographs or 2D imaging. Further studies are required to create the standard method for these measurements on 3D models, for example by taking into account the pelvic incidence and hip flexion and comparing them with the radiographs as the current reference standard. Another potential limiting factor in measuring LCEA on 3D images is the absence of whole pelvis imaging in a few of our cases. This limits the correction for pelvic tilt, which is required for improved reproducibility and accuracy of measurements [39, 40]. This limitation can be addressed in future studies by including whole pelvis in MRI image acquisition.

There are several limitations with our study, beginning with our small sample size. The concern over the additional cost and radiation related to the CT imaging has prompted the hip preservation orthopedic surgeons at our institution to decrease the number of CTs ordered, and only a small cohort of patients underwent both 3D-CT and MRI studies of the same hip. Second, our study lacks asymptomatic controls, as those patients selected for advanced imaging in our study had symptoms of impingement. Hip pain is a prerequisite for these patients for obtaining both CT and MRI of the same hip. It would be unethical to submit an asymptomatic patient to the ionizing radiation of a CT scan without a symptom. We acknowledge that there is selection bias in this study, as all patients selected for advanced imaging were screened by X-rays and evaluated for hip pain. Of note, previous studies have encountered these same limitations [20, 37, 41]. Third, we acknowledge that other parameters of FAI in the preoperative evaluation, such as femoral and acetabular retroversion, were not studied, mainly because of the technical limitations and lack of standard methodology.

Finally, there is currently support for advanced 3D hip models, mainly 3D-CT, for research and for potential use in more challenging FAI cases, such as revision FAI surgery [42]. With respect to the clinical outcome, future research can help to determine if adding advanced 3D hip imaging for pre-surgical planning can improve surgical outcomes for FAI patients compared with using 2D imaging and plain radiographs.

We have shown that 3D-MRI of the hip can be used to accurately diagnose and quantify the typical osseous pathological conditions in patients with FAI. These 3D MR

reconstructions have the potential to eliminate the need for 3D-CT imaging for this predominantly young group of patients, and its associated radiation exposure and cost.

Compliance with ethical standards

Conflicts of interest The authors declare that they have no conflicts of interest.

Disclosures None.

Institutional review board Institutional review board approval was obtained.

References

1. Bredella MA, Ulbrich EJ, Stoller DW, Anderson SE. Femoroacetabular impingement. Magn Reson Imaging Clin N Am. 2013;21:45–64.
2. Leunig M, Ganz R. Femoroacetabular impingement. A common cause of hip complaints leading to arthrosis. Unfallchirurg. 2005;108:9–10. 12–7.
3. Nötzli HP, Wyss TF, Stoecklin CH, Schmid MR, Treiber K, Hodler J. The contour of the femoral head-neck junction as a predictor for the risk of anterior impingement. J Bone Joint Surg Br. 2002;84:556–60.
4. Wagner S, Hofstetter W, Chiquet M, Mainil-Varlet P, Stauffer E, Ganz R, et al. Early osteoarthritic changes of human femoral head cartilage subsequent to femoro-acetabular impingement. Osteoarthritis Cartilage. 2003;11:508–18.
5. Ganz R, Parvizi J, Beck M, Leunig M, Nötzli H, Siebenrock KA. Femoroacetabular impingement: a cause for osteoarthritis of the hip. Clin Orthop Relat Res. 2003;(417):112–20.
6. Siebenrock KA, Wahab KHA, Werlen S, Kalhor M, Leunig M, Ganz R. Abnormal extension of the femoral head epiphysis as a cause of cam impingement. Clin Orthop Relat Res. 2004;(418):54–60.
7. Murphy S, Tannast M, Kim Y-J, Buly R, Millis MB. Debridement of the adult hip for femoroacetabular impingement: indications and preliminary clinical results. Clin Orthop Relat Res. 2004;(429):178–81.
8. Tanzer M, Noiseux N. Osseous abnormalities and early osteoarthritis: the role of hip impingement. Clin Orthop Relat Res. 2004;(429):170–7.
9. Beck M, Kalhor M, Leunig M, Ganz R. Hip morphology influences the pattern of damage to the acetabular cartilage: femoroacetabular impingement as a cause of early osteoarthritis of the hip. J Bone Joint Surg Br. 2005;87:1012–8.
10. Barros HJM, Camanho GL, Bernabé AC, Rodrigues MB, Leme LEG. Femoral head-neck junction deformity is related to osteoarthritis of the hip. Clin Orthop Relat Res. 2010;468(7):1920–5.
11. Tönnis D. Normal values of the hip joint for the evaluation of X-rays in children and adults. Clin Orthop Relat Res. 1976;(119):39–47.
12. Tannast M, Siebenrock KA, Anderson SE. Femoroacetabular impingement: radiographic diagnosis—what the radiologist should know. Am J Roentgenol. 2007;188:1540–52.
13. Clohisy JC, Carlisle JC, Beaulé PE, Kim Y-J, Trousdale RT, Sierra RJ, et al. A systematic approach to the plain radiographic evaluation of the young adult hip. J Bone Joint Surg Am. 2008;90(Suppl 4):47–66.
14. Domayer SE, Ziebarth K, Chan J, Bixby S, Mamisch TC, Kim YJ. Femoroacetabular cam-type impingement: diagnostic sensitivity and specificity of radiographic views compared to radial MRI. Eur J Radiol. 2011;80:805–10.
15. James SLJ, Ali K, Malara F, Young D, O'Donnell J, Connell DA. MRI findings of femoroacetabular impingement. AJR Am J Roentgenol. 2006;187:1412–9.
16. Pfirrmann CWA, Mengiardi B, Dora C, Kalberer F, Zanetti M, Hodler J. Cam and pincer femoroacetabular impingement: characteristic MR arthrographic findings in 50 patients. Radiology. 2006;240:778–85.
17. Nishihara S, Sugano N, Nishii T, Ohzono K, Yoshikawa H. Measurements of pelvic flexion angle using three-dimensional computed tomography. Clin Orthop Relat Res. 2003;(411):140–51.
18. Beaulé PE, Zaragoza E, Motamedi K, Copelan N, Dorey FJ. Three-dimensional computed tomography of the hip in the assessment of femoroacetabular impingement. J Orthop Res. 2005;23:1286–92.
19. Buller LT, Rosneck J, Monaco FM, Butler R, Smith T, Barsoum WK. Relationship between proximal femoral and acetabular alignment in normal hip joints using 3-dimensional computed tomography. Am J Sports Med. 2012;40:367–75.
20. Dandachli W, Najefi A, Iranpour F, Lenihan J, Hart A, Cobb J. Quantifying the contribution of pincer deformity to femoroacetabular impingement using 3D computerised tomography. Skeletal Radiol. 2012;41:1295–300.
21. Heyworth BE, Dolan MM, Nguyen JT, Chen NC, Kelly BT. Preoperative three-dimensional CT predicts intraoperative findings in hip arthroscopy. Clin Orthop Relat Res. 2012;470(7):1950–7.
22. Milone MT, Bedi A, Poultsides L, Magennis E, Byrd JWT, Larson CM, et al. Novel CT-based three-dimensional software improves the characterization of cam morphology. Clin Orthop Relat Res. 2013;471(8):2484–91.
23. Gyftopoulos S, Beltran LS, Yemin A, Strauss E, Meislin R, Jazrawi L, et al. Use of 3D MR reconstructions in the evaluation of glenoid bone loss: a clinical study. Skeletal Radiol. 2014;43:213–8.
24. Gyftopoulos S, Yemin A, Mulholland T, Bloom M, Storey P, Geppert C, et al. 3DMR osseous reconstructions of the shoulder using a gradient-echo based two-point Dixon reconstruction: a feasibility study. Skeletal Radiol. 2013;42:347–52.
25. Boese CK, Frink M, Jostmeier J, Haneder S, Dargel J, Eysel P, et al. The modified femoral neck-shaft angle: age- and sex-dependent reference values and reliability analysis. Biomed Res Int. 2016;2016:8645027.
26. Hetsroni I, Poultsides L, Bedi A, Larson CM, Kelly BT. Anterior inferior iliac spine morphology correlates with hip range of motion: a classification system and dynamic model. Clin Orthop Relat Res. 2013;471(8):2497–503.
27. Audenaert EA, Baelde N, Huysse W, Vigneron L, Pattyn C. Development of a three-dimensional detection method of cam deformities in femoroacetabular impingement. Skeletal Radiol. 2011;40:921–7.
28. Ross JR, Bedi A, Stone RM, Sibilsky Enselman E, Leunig M, Kelly BT, et al. Intraoperative fluoroscopic imaging to treat cam deformities. Am J Sports Med. 2014;42:1370–6.
29. Radetzki F, Saul B, Hagel A, Mendel T, Döring T, Delank KS, et al. Three-dimensional virtual simulation and evaluation of the femoroacetabular impingement based on "black bone" MRA. Arch Orthop Trauma Surg. 2015;135:667–71.
30. Chhabra A, Nordeck S, Wadhwa V, Madhavapeddi S, Robertson WJ. Femoroacetabular impingement with chronic acetabular rim fracture—3D computed tomography, 3D magnetic resonance imaging and arthroscopic correlation. World J Orthop. 2015;6:498–504.
31. Kutty S, Schneider P, Faris P, Kiefer G, Frizzell B, Park R, et al. Reliability and predictability of the centre-edge angle in the assessment of pincer femoroacetabular impingement. Int Orthop. 2012;36:505–10.
32. Lequesne M, Malghem J, Dion E. The normal hip joint space: variations in width, shape, and architecture on 223 pelvic radiographs. Ann Rheum Dis. 2004;63:1145–51.

33. Harris-Hayes M, Royer NK. Relationship of acetabular dysplasia and femoroacetabular impingement to hip osteoarthritis: a focused review. PM R. 2011;3:1055–1067.e1.
34. Birrell F, Silman A, Croft P, Cooper C, Hosie G, Macfarlane G, et al. Syndrome of symptomatic adult acetabular dysplasia (SAAD syndrome). Ann Rheum Dis. 2003;62:356–8.
35. Gosvig KK, Jacobsen S, Sonne-Holm S, Palm H, Troelsen A. Prevalence of malformations of the hip joint and their relationship to sex, groin pain, and risk of osteoarthritis. J Bone Joint Surg Am Vol. 2010;92:1162–9.
36. Jacobsen S, Sonne-Holm S, Søballe K, Gebuhr P, Lund B. Joint space width in dysplasia of the hip: a case-control study of 81 adults followed for ten years. J Bone Joint Surg Br Vol. 2005;87–B:471–7.
37. Bouma HW, Hogervorst T, Audenaert E, Krekel P, van Kampen PM. Can combining femoral and acetabular morphology parameters improve the characterization of femoroacetabular impingement? Clin Orthop Relat Res. 2015;473:1396–403.
38. Ng KCG, Lamontagne M, Adamczyk AP, Rahkra KS, Beaulé PE. Patient-specific anatomical and functional parameters provide new insights into the pathomechanism of cam FAI. Clin Orthop Relat Res. 2015;473(12):1289–96.
39. Lohan DG, Seeger LL, Motamedi K, Hame S, Sayre J. Cam-type femoral-acetabular impingement: is the alpha angle the best MR arthrography has to offer? Skeletal Radiol. 2009;38:855–62.
40. Dandachli W, Ul Islam S, Tippett R, Hall-Craggs MA, Witt JD. Analysis of acetabular version in the native hip: comparison between 2D axial CT and 3D CT measurements. Skeletal Radiol. 2011;40:877–83.
41. Harris MD, Reese SP, Peters CL, Weiss JA, Anderson AE. Three-dimensional quantification of femoral head shape in controls and patients with cam-type femoroacetabular impingement. Ann Biomed Eng. 2013;41:1162–71.
42. Cadet ER, Babatunde OM, Gorroochurn P, Chan AK, Stancato-Pasik A, Brown M, et al. Inter- and intra-observer agreement of femoroacetabular impingement (FAI) parameters comparing plain radiographs and advanced, 3D computed tomographic (CT)-generated hip models in a surgical patient cohort. Knee Surg Sports Traumatol Arthrosc. 2016;24:2324–31.